Lawrence Berkeley National Laboratory
LBL Publications

Title
Impact of tropical cyclones on modeled extreme wind-wave climate

Permalink
https://escholarship.org/uc/item/1546k590

Journal
Geophysical Research Letters, 44(3)

ISSN
0094-8276

Authors
Timmermans, Ben
Stone, Dáithí
Wehner, Michael
et al.

Publication Date
2017-02-16

DOI
10.1002/2016gl071681

Peer reviewed

eScholarship.org Powered by the California Digital Library
University of California

AGU PUBLICATIONS

Geophysical Research Letters

RESEARCH LETTER

10.1002/2016GL071681

Key Points:
- The effect of increased forcing wind resolution on simulated global wave height extremes is quantified
- 20-year return levels for wave height return levels are highly dependent on resolution in tropical cyclone regions and sensitive to sampling
- Simulations of a future RCP 8.5 scenario suggest large increases in extreme waves in some areas

Supporting Information:
- Texts S1 and S2 and Figures S1–S16

Correspondence to:
B. Timmermans,
bwtimmermans@lbl.gov

Citation:
Timmermans, B., D. Stone, M. Wehner, and H. Krishnan (2017), Impact of tropical cyclones on modeled extreme wind-wave climate, *Geophys. Res. Lett.*, *44*, 1393–1401, doi:10.1002/2016GL071681.

Received 25 OCT 2016
Accepted 15 JAN 2017
Accepted article online 19 JAN 2017
Published online 4 FEB 2017

©2017. American Geophysical Union. All Rights Reserved.

Impact of tropical cyclones on modeled extreme wind-wave climate

Ben Timmermans[1], Dáithí Stone[1], Michael Wehner[1], and Harinarayan Krishnan[1]

[1] Lawrence Berkeley National Laboratory, Berkeley, California, USA

Abstract The effect of forcing wind resolution on the extremes of global wind-wave climate are investigated in numerical simulations. Forcing winds from the Community Atmosphere Model at horizontal resolutions of ~1.0° and ~0.25° are used to drive Wavewatch III. Differences in extreme wave height are found to manifest most strongly in tropical cyclone (TC) regions, emphasizing the need for high-resolution forcing in those areas. Comparison with observations typically show improvement in performance with increased forcing resolution, with a strong influence in the tail of the distribution, although simulated extremes can exceed observations. A simulation for the end of the 21st century under a RCP 8.5 type emission scenario suggests further increases in extreme wave height in TC regions.

1. Introduction

Wind-waves on the ocean are a familiar natural phenomenon that directly affects coastal communities, offshore industries, and shipping. Wave-related impacts can be severe [*Hoeke et al.*, 2013], so naturally there is a growing interest in the evolution of the wind-wave climate under climate change, noted in particular by the Intergovernmental Panel on Climate Change (IPCC) [*Field et al.*, 2014], which motivates efforts such as the Coordinated Wave Climate Intercomparison Project (COWCLIP) [*Hemer et al.*, 2012]. Wave climate research typically involves the generation of atmospheric variables, often near surface winds, using a global circulation model (GCM) that can then be used to derive ocean waves either statistically [*Wang and Swail*, 2006] or numerically [*Hemer et al.*, 2013a; *Fan et al.*, 2013]. Downscaling approaches from historical and reanalysis data are also used [*Camus et al.*, 2014]. Environmental and societal impacts of weather and climate are typically associated with the largest magnitude events—the extremes—and a number of studies have considered the extremes of wave climate [*Wang et al.*, 2014; *Mori et al.*, 2010; *Shimura et al.*, 2015]. However, investigation of extremes through numerical modeling is challenging. Long time series of output are required in order to make inferences about extreme events, ensembles of which are generally desirable in order to evaluate uncertainties. Furthermore, limitations of the model, such as numerical resolution, affect its ability to accurately reproduce the physical processes responsible for extreme phenomena. Specifically, severe storms, including TCs, generate the most extreme waves in affected regions but are not well resolved at available spatial and temporal resolutions. Each of these issues increases the computational burden.

Waves are generated from wind stress on the ocean surface, and clearly stronger storms generate larger waves. However, variables like storm size, intensity, structure, and translation speed combine to create different wave conditions, and each of these is a function of resolution. For example, midlatitude storms tend to be spatially broad and well resolved at 1.0° and better. While they lack the extreme wind speeds of intense TCs (up to ~55 m s^{-1}), average speeds can be high (~20 m s^{-1}), they are more frequent, and fast moving storms in the absence of a land boundary (such as in the Southern Ocean) result in very long effective fetch, allowing for the evolution of very large waves. By contrast, an intense tropical cyclone (TC) is spatially more constrained, typically generating extreme waves locally, at much shorter fetch, from the extreme winds close (~100 km) to the eyewall. Given the strong dependence of simulations of TCs on resolution, it is clear that the wave climate, particularly in the extremes, will be sensitive to forcing resolution.

To date, most available climate model data sets, e.g., those submitted to the Coupled Model Intercomparison Project phase 5 (CMIP5) [*Taylor et al.*, 2012], are at horizontal resolutions of approximately 1.0° (~100 km), and temporal resolutions of 6 h. Given that this is too low to create realistic TCs [*Wehner et al.*, 2015], and given their importance to the tail of the wind speed distribution, reliable characterization of extreme waves in affected regions is not possible [*Breivik et al.*, 2014]. Studies of wind-wave climate based on lower resolution

Table 1. Wind Data Sets From CAM5, Used to Force WW3

Resolution (lat. × lon. deg)	Time Step (h)	Total Duration (years)	Scenario	Details
0.9 × 1.25	3	53	Present day	Single continuous run (1960 to 2012)
			ALL-HIST	Observed SSTs
0.23 × 0.31	3	44	Present day	11 year runs (1995 to 2005)
			ALL-HIST	Four-member ensemble (44 years total)
				Runs initialized with perturbed physics
				Observed SSTs
0.23 × 0.31	3	23	Future RCP 8.5	1 × 19 year run (2081 to 2099)
				4 additional years (2080 to 2083)
				Runs initialized with perturbed physics
				Observed SSTs + 2°C
				Doubled atmospheric CO_2

simulations therefore lack the influence of TCs [*Hemer et al.*, 2013b; *Wang et al.*, 2014; *Erikson et al.*, 2015]. With more recent availability of sufficient computing resource to simulate climate at higher resolution, detailed investigation of TC climatology is possible [*Strachan et al.*, 2013; *Murakami et al.*, 2015]. Consequently, studies of wind-wave climate that capture more explicitly the effects of TCs are also appearing in the literature [*Fan et al.*, 2013; *Shimura et al.*, 2015]. However, with a sparsity of research in this area, and studies employing different approaches, sources of uncertainty and their importance remain poorly understood. In particular, we note that no study specifically obviates and quantifies the impact of increased resolution for wind-wave climate research.

We address this issue by making use of output from recent high-resolution atmospheric simulations. The atmospheric component of the Community Earth System Model, the Community Atmosphere Model version 5.1 (CAM5) [*Neale et al.*, 2010], has been shown to generate realistic TCs at a horizontal resolution of approximately 0.25° (~25 km) [*Wehner et al.*, 2014; *Bacmeister et al.*, 2014; *Wehner et al.*, 2015]. Several decades of global climatic variables from CAM5 at this resolution and at 3-hourly time steps have been generated, and we describe the results from using this output to force the numerical global wave model Wavewatch III (WW3) [*Tolman*, 2014]. We present three global wave data sets at 0.25° resolution. Two of these represent present day conditions and are forced by winds at approximately 1.0° and 0.25° (referred to as low resolution and high resolution, respectively). We focus primarily on differences between these two cases in terms of extreme significant wave height (H_s). Following *Wang et al.* [2014], we make use of extreme value theory and express the extremes in terms of 20-year return levels. Large differences in regions affected by TCs are identified, highlighting the importance of forcing resolution in such research. A third data set uses high-resolution forcing winds under a future RCP 8.5 emission scenario at the end of the 21st century, and we evaluate possible future changes in extremes. Sources of uncertainty are not formally addressed beyond the statistical uncertainty arising from the fitting of extreme value distributions.

The structure of this paper is therefore as follows. In section 2 we describe the numerical modeling and statistical methods used. Section 3 gives a summary of the performance of the wave model with respect to observations. Sections 4 and 5 present the results for wave statistics and return levels, respectively, and in section 6 we give further discussion and concluding remarks.

2. Methods

Three time series of global forcing winds simulated with CAM5 were used to generate waves with WW3. Details are given in Table 1. Further discussion of the simulation of these winds is given in section 2.1. Further details of the configuration of WW3 is given in section 2.2. All statistical analysis that has been performed is per grid cell, with no further spatial or temporal downscaling.

2.1. Atmospheric Simulations

CAM5 models the three-dimensional dynamics and thermodynamics of the atmosphere and land surface [*Neale et al.*, 2010], and has been shown to generate realistic TCs when run at ~0.25° horizontal resolution. Details of the configuration and its ability to generate intense TCs are given in *Bacmeister et al.* [2014] and *Wehner et al.* [2015]. Since CAM5 lacks ocean coupling, observed sea surface temperature (SST) boundary conditions were specified following *Hurrell et al.* [2008]. Daily values are obtained from linear interpolation of monthly averages. For RCP 8.5 future runs, SSTs were derived from observed values, and modified by adding 2°C uniformly across the spatial domain.

2.2. Numerical Wave Modeling

WW3 [*Tolman*, 2014] models the time evolution of phase-averaged wave energy spectrum over the global ocean surface. For all simulations, WW3 was run on a global grid at 0.25°. Standard wave summary statistics (such as H_s) were obtained at 3-hourly intervals as global fields. Note that only fields for H_s are presented in this work. Further details of model configuration are described in Text S1 of the supporting information.

To expedite computation, years were run in parallel, which introduced discontinuities into the time series that could affect the passage of swell over long distances. However, extreme wave conditions tend to arise from local wind-sea interactions during a storm and typically evolve in less than 24 h, so we judge the impact to be small. To mitigate this problem, WW3 was "spun-up" by running the final week of the previous year at the start of each simulation.

The suitability of WW3 to investigate extremes is not discussed in this paper, although we acknowledge that phase-averaged wave models are based upon assumptions which do not hold in extreme sea states. However, performance can be good [*Moon et al.*, 2003], to the extent that WW3, appropriately configured, is used for operational hurricane wave forecasting by the U.S. National Oceanic and Atmospheric Administration [*Chao and Tolman*, 2010]. A discussion of the comparison of simulated and observed wave height statistics is given in section 3.

2.3. Extreme Value Analysis

We make use of extreme value theory to describe the extremes of H_s. We assume that each year is an independent sample from a stationary time series and fit a point process to each spatial grid point by sampling peaks over a high threshold (POT) [see, e.g., *Davison and Smith*, 1990; *Coles*, 2001]. Each point process was fitted through maximum likelihood estimation resulting in a parameterized generalized Pareto extreme value distribution (EVD). In this paper we describe the extremes of H_s in terms of the 20-year return level, determined from the fitted EVDs. Confidence intervals can be obtained for the return level estimates, which provides a basis for statistical inference, but note that the confidence intervals capture only sampling uncertainty and we do not formally address other sources of uncertainty in this work. More details of fitting the EVDs is given in Text S2.

3. Simulation Performance

With our focus on the impact of resolution increase, we provide only a limited examination of the performance of simulations with respect to observations. We do so graphically, by using Q-Q plots to compare distributions of simulated wave height with observations from various NOAA data buoys (http://www.ndbc.noaa.gov/). Details of the buoys are shown in Figure S1, and a representative example of a comparison outside and inside a TC zone is shown in Figure 1. Additional locations are shown in Figures S2 to S7. For comparison, Q-Q plots for wind speed at all buoys are provided in Figures S8 and S9. There is clear correspondence between wind speed and wave height distributions, but we do not discuss wind speed further at this point.

We primarily identify the difference in the impact of resolution increase between those locations inside and outside TC-affected regions. Specifically, simulations in extratropical cyclone (ETC) regions seem largely unaffected by increased resolution. Figures 1a and 1b show comparisons of simulation with observations at NDBC 46066. The 0.5, 0.9, 0.99, 0.999, and 0.9999 quantiles are indicated by red dashed lines. In general, there is very good agreement at both resolutions, and similar results can be seen for NDBC 46006 (Figure S2), also predominantly affected by ETCs.

Results in locations affected by TCs show more varied performance, for example, at NDBC 41002 in the North Atlantic, shown in Figures 1c and 1d. There is a trend of underprediction at quantiles below 0.999 although less pronounced in the high-resolution case. However, above the 0.999 quantile, correspondence

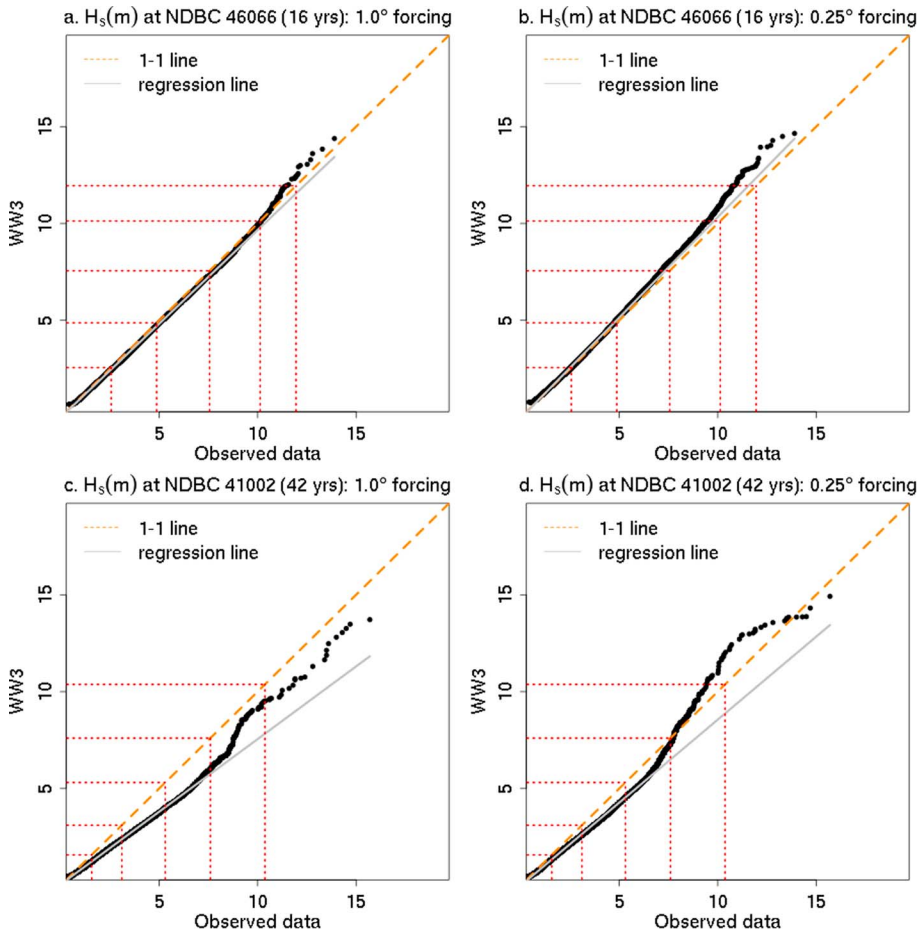

Figure 1. Q-Q plots of observed versus simulated H_s at NOAA data buoys (a, b) 46066, and (c, d) 41002. Note that the duration, in years, in the panel titles indicates the number of years of observations at the buoy. This typically differs from the simulation length.

varies, with simulated waves tending to exceed observations. Comparisons for other data buoys (Figures S2 to S7) reveal similar features. In particular, we see dramatic increases in the tail of the distribution, consistent with better representation of extreme winds from TCs. In many cases improved agreement with observations at lower quantiles is evident. Also, often seen is a distinct change in the gradient of the Q-Q line (see, e.g., Figures 1d and S3b), which could be indicative of a transition from prevailing conditions to TC waves. Apparent overestimation of extremes in some locations, in particular, NDBC 42001 (Gulf of Mexico) and NDBC 41047 (North Atlantic), may be due to a number of sources of error, but we speculate that poor spatiotemporal sampling of TCs and resulting waves is at least partly responsible. Their narrow storm tracks and infrequent passage, together with the limited duration of data sets, and the sensitivity of extreme waves to the close passage of TCs, likely give rise to different tail characteristics when distributions are compared. This issue is discussed further in section 6.

4. Comparison of Overall Statistics

Statistics (mean, 99.9th percentile and maximum) from the low resolution (Figures 2a–2c) and differences between low- and high-resolution forcing (Figures 2d–2f) are compared. A common scale is used, which reveals an order of magnitude difference between the mean and most extreme waves in the tropics and extratropics. Differences between the two resolutions are not obvious until we consider very high quantiles. At the 99.9th percentile (Figure 2e), differences can be seen, for example, to the west of Mexico and south of Japan—areas affected by TCs. When considering the difference in maximum H_s (Figure 2f), however, individual storm tracks can be seen in areas affected by TCs. Wave patterns arising from TC-like phenomena in the low-resolution case are broader in spatial extent and less frequent, consistent with differences in TC behavior

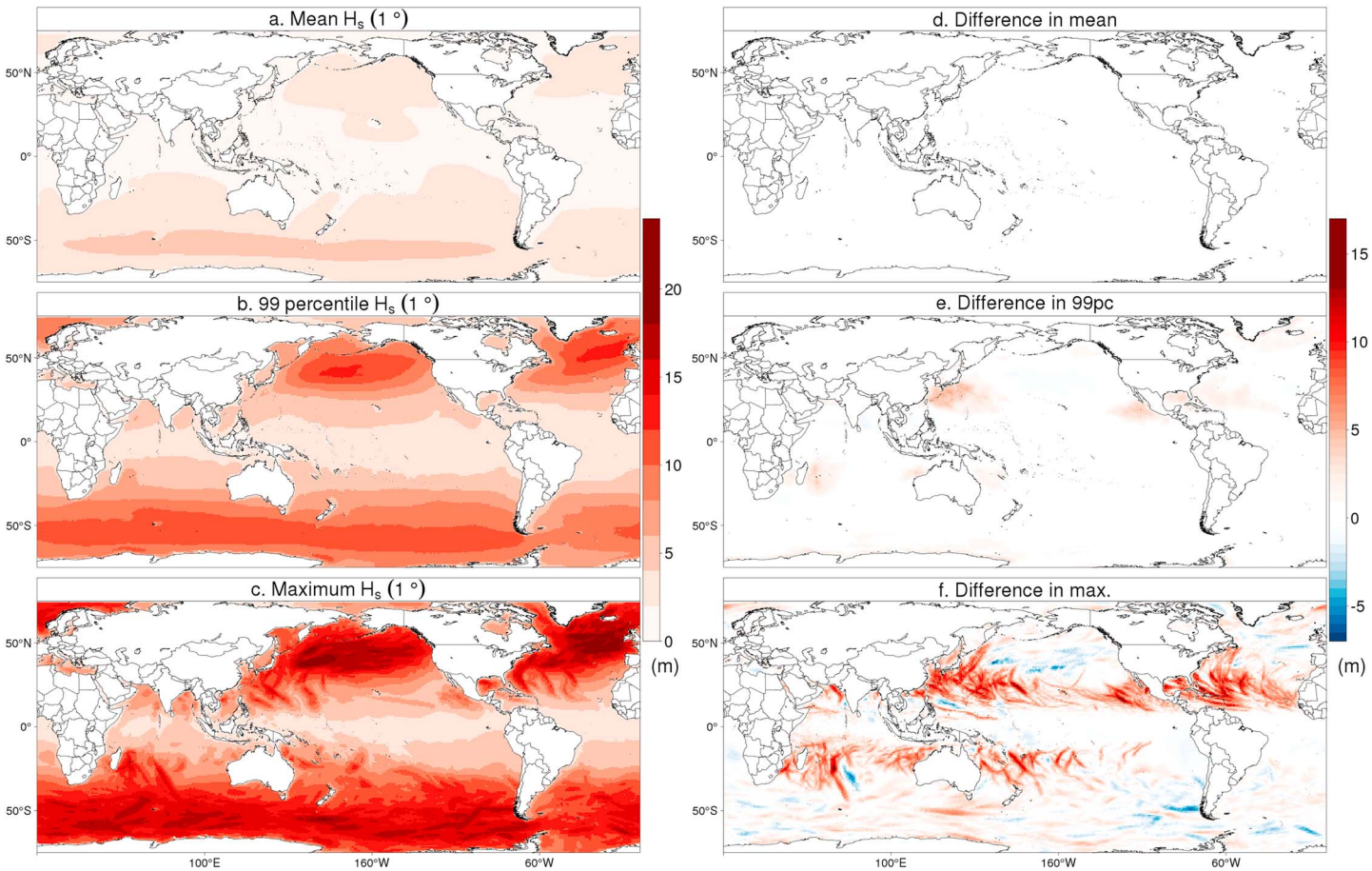

Figure 2. (a) Mean, (b) 99.9th percentile, and (c) maximum H_s generated from forcing winds at 1.0° and (d–f) differences between output from forcing at 0.25°.

between the two resolutions [*Wehner et al.*, 2015]. Other general features such as waves from extratropical storms in the Southern Ocean appear to differ little between the runs.

Very poor sampling of extreme events is evidenced by single storm tracks passing through areas with otherwise benign conditions. This is particularly apparent just north and south of the equator and also off the northeast and northwest coasts of Australia, for example. Note that wave height distributions at such locations are characterized by very heavy tails—perhaps a single severe event ($H_s > 10$ m), at a location where the maximum would otherwise be much lower ($H_s \ll 6$ m). This has implications for the fitting of EVDs, which are discussed in Text S2. Maps of global statistics for the future time series are not shown but are qualitatively similar.

5. Comparison of Return Levels

To examine the extremes, we derived 20-year return levels for H_s by fitting EVDs to the time series at each grid point. The influence of TCs gives rise to a range of H_s distributions with both "short" and "long" tails, requiring flexibility in the fitting process. Further details are provided in Text S2. We use the fitted EVDs to derive 20-year return levels, shown for 0.25° present day in Figure 3a. Differences between return values from 0.25° and 1.0° forcing (present day) and future and present (at 0.25°) are shown in Figures 3b and 3c, respectively. In Figures 3b and 3c, speckled shading indicates where the difference in the estimated return level exceeds three times the combined standard deviation of the two return level estimates. This can be interpreted as a measure of confidence in the results with respect to the goodness of fit of the EVD. We emphasize that only sampling uncertainty contributes to the confidence intervals, and other important sources of uncertainty are not analyzed here.

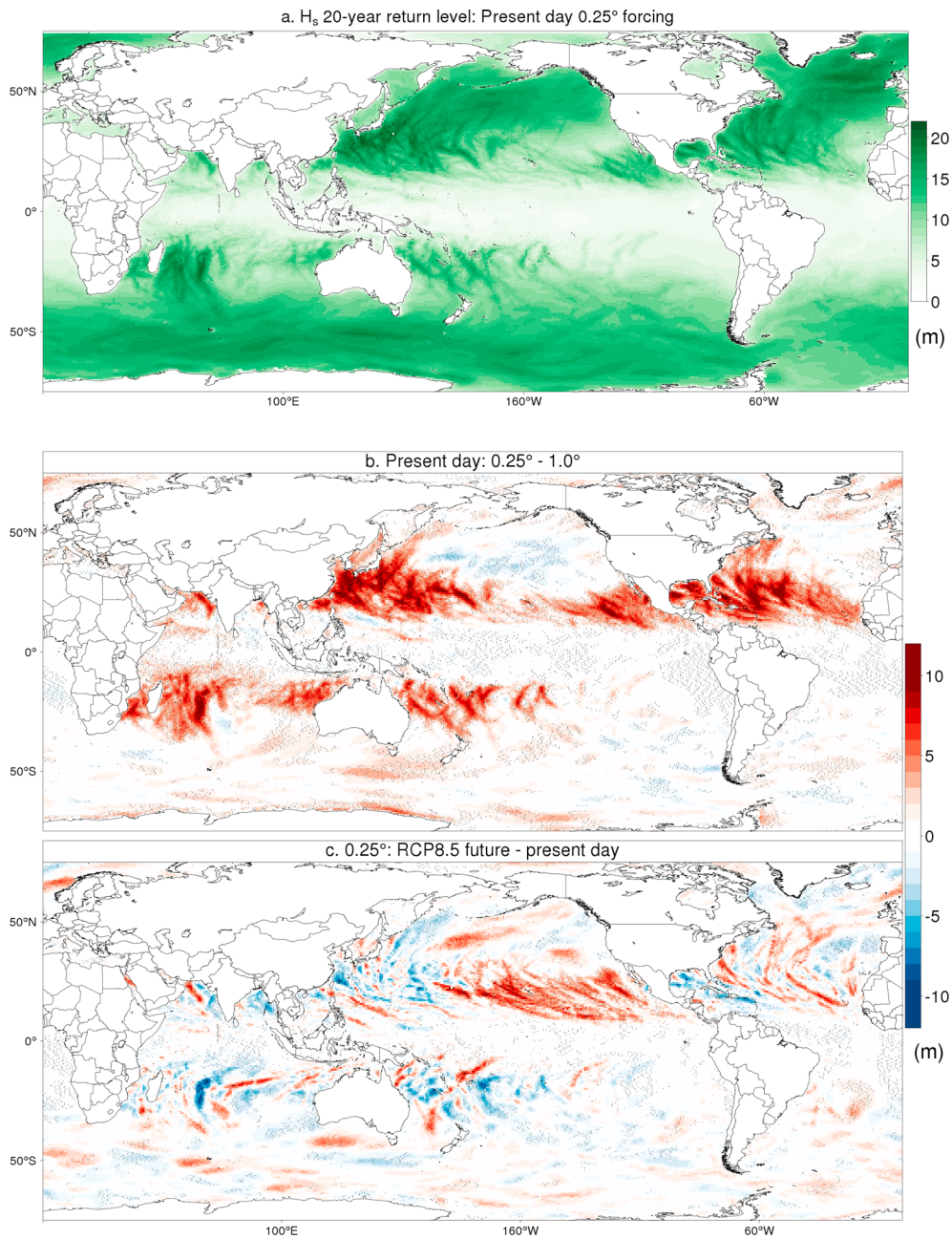

Figure 3. (a) H_s 20-year return level computed from 0.25° forcing for present-day conditions, with (b) differences between 1.0° and 0.25° forcing for present day conditions and (c) differences between present-day and future RCP 8.5 conditions at 0.25° forcing.

5.1. Present Day, Forcing at 1.0° Versus 0.25°

Figure 3a shows that 20-year return levels are strongly influenced by the passage of individual storms and, consistent with Figure 2f, Figure 3b reveals that large regions of the globe show significant differences between the two data sets. In particular, the higher resolution forcing strongly affects estimation of the extremes in the TC affected areas. Differences of up to 10 m in 20-year return levels highlight the absence of large waves in TC regions when using the 1.0° forcing. We caution the interpretation of the absolute differences in return level owing to the presence of uncertainties, as discussed in section 3. However, the figure serves to show that there is a systematic and positive effect on extreme wave heights clearly consistent with TC regions. Additionally, there appears to be a small increase in the Southern Ocean and a small decrease in the northern Pacific ETC region.

5.2. Forcing at 0.25°, Present Day Versus Future RCP 8.5

Considering Figure 3c, the difference between present and future wave extremes appears less clear. Statistical difference indicated by the speckled pattern is far less contiguous and covers much less of the globe than in Figure 3b, suggesting larger uncertainty and smaller differences in estimate. Moreover, the effect of individual storm tracks is evident in both TC and ETC zones, and large differences both positive and negative, appear to arise solely due to the passage (or otherwise) of a single large storm over a particular area. For example, we can infer that in the future RCP 8.5 data set a powerful hurricane passed through the middle of the North Atlantic. Variability in the sign of change is prevalent in all regions with the exception of the TC zone directly to the west of Mexico. An apparent shift of TC activity to the west gives rise to a large increase in extreme wave height in that region. Noting the short (23 year) time series, it is presumptuous to draw strong conclusions in the absence of more data.

6. Discussion

The large differences in 20-year return levels highlight the importance of wind resolution in extreme wave climate research and are consistent with superior representation of TCs in higher resolution atmospheric data sets. It is encouraging that comparison of simulations with observations suggests that in many areas increase in resolution leads to improved reproduction of H_s statistics, both average and extreme. Outside TC regions, change in extremes attributable to increased resolution tends to be much smaller, if any. Although the high-resolution forcing has a strong effect in the tail of the H_s distribution, comparison with observations reveals a spatially varying correspondence that is poor in some locations. A number of sources of uncertainty might be responsible for the disagreement, which include poor sampling (discussed below), coarse winds, and the lack of ocean-atmosphere feedback, which also affects SST patterns. The 3-hourly winds used here are state of the art for global modeling, but they are sufficiently temporally coarse to be an appreciable source of error. In addition, wind-wave-ocean interactions are complex and without multiway coupling of models, the accuracy of wave predictions is likely limited [*Moon et al.*, 2004]. SST pattern is also an important source of uncertainty that has been investigated by others (discussed shortly). The use of observed SSTs, for example, captures the signature of atmospheric oscillations, and TCs, that actually took place, potentially introducing bias and leading to an underestimate of variability. While these are important considerations, we suggest that uncertainty due to spatiotemporal sampling of TCs and resulting waves, appears to dominate our results. This affects both the assessment of performance, and the analysis of future changes in extreme wave climate. We can see from Figure 2f, that at higher resolution, TC tracks are better defined and spatially narrow. Since TCs occur infrequently (<30 annually), a long sampling duration is required to obtain an estimate of the limiting spatial distribution of the resulting extreme waves. However, with sample sizes typically shorter than 50 years, comparison of extremes at a point location (e.g., Figure 1) is heavily influenced by the chance passage of a storm in one data set, and not the other. Equivalently, this affects the analysis of future change, shown in Figure 3, where individual storm tracks are evident. To minimize expensive model runs and make efficient use of the available data, we suggest the application of a spatial statistical approach for extremes [see, e.g., *Northrop and Jonathan*, 2011; *Davison and Huser*, 2015].

Although simulation performance requires further investigation, the strength of response in the tail of the H_s distribution in TC zones suggests that the "step-up" to 0.25° could prove sufficient for reliable global analysis of extreme waves (including TC regions). That is, reduction in uncertainty, or error, from resolutions better than 0.25°, may be sufficiently small compared to other important sources (such as sampling or future SSTs), that increase in resolution beyond 0.25° could remain unjustified for some time—especially noting the enormous cost. If this is the case, it would serve as motivation to focus research effort on obtaining longer-duration samples at similar resolutions and developing efficient statistical methods. Further improvement in performance may be readily achievable through temporal interpolation of the wind, or wave model tuning, both of which are practical to investigate.

Recent studies that examine projections of extreme waves highlight the importance of other sources of uncertainty. *Shimura et al.* [2015] and *Fan et al.* [2013] focus on future changes in wave climate by considering the IPCC A1B scenario (comparable to RCP 8.5) at the end of the 21st century. Although different methodologies were employed, in both cases ensembles of global wave climatologies were generated numerically from forcing winds at resolutions of approximately 0.5°, which can produce TCs. Ensemble members were derived from different SST patterns and physical parameterizations. In both cases, changes in extreme wave heights were examined (annual maxima and 0.99 quantile, respectively), and global maps of future extreme

wave height anomaly were generated (their Figures 5, and 8, respectively). There is substantial spatial variation in wave height anomaly between ensemble members, indicating the magnitude of uncertainty due to SST pattern and model physics. Making a qualitative comparison with our results, the most dramatic future change we identify is the strengthening of TC waves west of Mexico, seen clearly in Figure 3c. Similar spatial patterns are exhibited by individual ensemble members shown in both *Shimura et al.* [2015] and *Fan et al.* [2013], Figure 5(l) and figure 8(h), respectively. However, variability between members suggests that wave climate reflects strongly the characteristics of the atmospheric forcing (influenced by SST patterns and model physics), and it remains unclear whether the features of our atmospheric data set, that manifest strongly in the extreme wave climate, are significant.

Finally, we believe a valuable extension to this work would be to rigorously determine the effect of TC characteristics as a function of resolution, such as storm size distribution, on wave climate. A more detailed investigation might require the identification of individual storms and could incorporate a multivariate analysis by considering wave period and direction [*Shimura et al.*, 2015]. We do already have a sense of the change in storm size distribution. *Wehner et al.* [2015] show that, at 1.0°, hurricanes do not exceed category 2 on the Saffir-Simpson scale but that weaker storms are too frequent, revealing a lack of extremes and suggesting an excessive density of high, but not extreme, winds. At 0.25°, however, the overall distribution of TCs is more realistic, including category 5 hurricanes in the appropriate numbers. Identification of all relevant storms and their climatology (using machine learning techniques [*Prabhat et al.*, 2012]), together with a multivariate analysis of wave data (height, period, etc.), could yield a much more robust description of the relationship between resolution, storm size, and wave climate.

Acknowledgments
This material is based upon work supported by the Regional and Global Climate Modeling Program of the U.S. Department of Energy, Office of Science, Office of Biological and Environmental Research, under contract DE-AC02-05CH11231. Calculations were performed at the National Energy Research Supercomputing Center (NERSC) at the Lawrence Berkeley National Laboratory where the data from these simulations are archived and available from the authors. All observational wave data were obtained from the National Oceanographic and Atmospheric Administration at http://www.ndbc.noaa.gov/. Data generated to support this work are available on request to the corresponding author (bwtimmermans@lbl.gov).

This manuscript has been authored by an author at Lawrence Berkeley National Laboratory, under Contract No. DE-AC02-05CH11231 with the U.S. Department of Energy. The U.S. Government retains, and the publisher, by accepting the article for publication, acknowledges, that the U.S. Government retains a non-exclusive, paid-up, irrevocable, world-wide license to publish or reproduce the published form of this manuscript, or allow others to do so, for U.S. Government purposes.

References

Ardhuin, F., et al. (2010), Semiempirical dissipation source functions for ocean waves. Part I: Definition, calibration, and validation, *J. Phys. Oceanogr.*, *40*, 1917–1941, doi:10.1175/2010JPO4324.1.

Bacmeister, J. T., M. F. Wehner, R. B. Neale, A. Gettelman, C. Hannay, P. H. Lauritzen, J. M. Caron, and J. E. Truesdale (2014), Exploratory high-resolution climate simulations using the Community Atmosphere Model (CAM), *J. Clim.*, *27*, 3073–3099, doi:10.1175/JCLI-D-13-00387.1.

Breivik, Ø., O. J. Aarnes, S. Abdalla, J.-R. Bidlot, and P. A. Janssen (2014), Wind and wave extremes over the world oceans from very large ensembles, *Geophys. Res. Lett.*, *41*, 5122–5131, doi:10.1002/2014GL060997.

Camus, P., M. Menéndez, F. J. Méndez, C. Izaguirre, A. Espejo, V. Cánovas, J. Pérez, A. Rueda, I. J. Losada, and R. Medina (2014), A weather-type statistical downscaling framework for ocean wave climate, *J. Geophys. Res. Oceans*, *119*, 7389–7405, doi:10.1002/2014JC010141.

Chao, Y. Y., and H. L. Tolman (2010), Performance of NCEP regional wave models in predicting peak sea states during the 2005 North Atlantic hurricane season, *Weather Forecasting*, *25*, 1543–1567, doi:10.1175/2010WAF2222309.1.

Coles, S. (2001), *An Introduction to Statistical Modeling of Extreme Values*, Springer, London.

Davison, A., and R. Huser (2015), Statistics of extremes, *Annu. Rev. Stat. Appl.*, *2*, 203–235, doi:10.1146/annurev-statistics-010814-020133.

Davison, A. C., and R. L. Smith (1990), Models for exceedances over high thresholds, *J. R. Stat. Soc. B*, *52*, 393–442.

Erikson, L., C. Hegermiller, P. Barnard, P. Ruggiero, and M. van Ormondt (2015), Projected wave conditions in the Eastern North Pacific under the influence of two CMIP5 climate scenarios, *Ocean Modell.*, *96*, 171–185, doi:10.1016/j.ocemod.2015.07.004.

Fan, Y., I. M. Held, S.-J. Lin, and X. L. Wang (2013), Ocean warming effect on surface gravity wave climate change for the end of the twenty-first century, *J. Clim.*, *26*, 6046–6066, doi:10.1175/JCLI-D-12-00410.1.

Field, C., et al. (Eds.) (2014), *IPCC, 2014: Climate Change 2014: Impacts, Adaptation, and Vulnerability. Part A: Global and Sectoral Aspects. Contribution of Working Group II to the Fifth Assessment Report of the Intergovernmental Panel on Climate Change*, Cambridge Univ. Press, Cambridge, U. K.

Hasselmann, S., K. Hasselmann, J. H. Allender, and T. P. Barnett (1985), Computation and parameterizations of the nonlinear transfer of energy in gravity-wave part 2: Parameterizations of the nonlinear energy transfer for application in wave models, *J. Phys. Oceanogr.*, *15*, 1378–1391.

Hemer, M. A., X. L. Wang, R. Weisse, and V. R. Swail (2012), Advancing wind-waves climate science: The COWCLIP project, *Bull. Am. Meteorol. Soc.*, *93*, 791–796, doi:10.1175/BAMS-D-11-00184.1.

Hemer, M. A., J. Katzfey, and C. E. Trenham (2013a), Global dynamical projections of surface ocean wave climate for a future high greenhouse gas emission scenario, *Ocean Modell.*, *70*, 221–245, doi:10.1016/j.ocemod.2012.09.008.

Hemer, M. A., Y. Fan, N. Mori, A. Semedo, and X. L. Wang (2013b), Projected changes in wave climate from a multi-model ensemble, *Nat. Clim. Change*, *3*, 471–476.

Hoeke, R. K., K. L. McInnes, J. C. Kruger, R. J. McNaught, J. R. Hunter, and S. G. Smithers (2013), Widespread inundation of Pacific islands triggered by distant-source wind-waves, *Global Planet. Change*, *108*, 128–138, doi:10.1016/j.gloplacha.2013.06.006.

Hurrell, J. W., J. J. Hack, D. Shea, J. M. Caron, and J. Rosinski (2008), A new sea surface temperature and sea ice boundary dataset for the Community Atmosphere Model, *J. Clim.*, *21*, 5145–5153, doi:10.1175/2008JCLI2292.1.

Moon, I.-J., I. Ginis, T. Hara, H. L. Tolman, C. W. Wright, and E. J. Walsh (2003), Numerical simulation of sea surface directional wave spectra under hurricane wind forcing, *J. Phys. Oceanogr.*, *33*, 1680–1706.

Moon, I.-J., I. Ginis, and T. Hara (2004), Effect of surface waves on air-sea momentum exchange. Part II: Behavior of drag coefficient under tropical cyclones, *J. Atmos. Sci.*, *61*, 2334–2348.

Mori, N., T. Yasuda, H. Mase, T. Tom, and Y. Oku (2010), Projection of extreme wave climate change under global warming, *Hydrol. Res. Lett.*, *4*, 15–19, doi:10.3178/HRL.4.15.

Murakami, H., et al. (2015), Simulation and prediction of category 4 and 5 hurricanes in the high-resolution GFDL HiFLOR coupled climate model, *J. Clim.*, *28*, 9058–9079, doi:10.1175/JCLI-D-15-0216.1.

Neale, R. B., et al. (2010), Description of the NCAR community atmosphere model (CAM 5.0), *Tech. Rep. NCAR Tech. Note NCAR/TN-486+ STR*, Natl. Cent. for Atmos. Res., Boulder, Colo.

Northrop, P. J., and P. Jonathan (2011), Threshold modelling of spatially dependent non-stationary extremes with application to hurricane-induced wave heights, *Environmentrics*, *22*, 799–809, doi:10.1002/env.1106.

Prabhat, O. R., S. Byna, K. Wu, F. Li, M. Wehner, and W. Bethel (2012), TECA: A parallel toolkit for extreme climate analysis, *Procedia Comput. Sci.*, *9*, 866–876, doi:10.1016/j.procs.2012.04.093.

Shimura, T., N. Mori, and H. Mase (2015), Future projections of extreme ocean wave climates and the relation to tropical cyclones: Ensemble experiments of MRI-AGCM3.2H, *J. Clim.*, *28*, 9838–9856.

Strachan, J., P. L. Vidale, K. Hodges, M. Roberts, and M.-E. Demory (2013), Investigating global tropical cyclone activity with a hierarchy of AGCMs: The role of model resolution, *J. Clim.*, *26*, 133–152, doi:10.1175/JCLI-D-12-00012.1.

Taylor, K. E., R. J. Stouffer, and G. A. Meehl (2012), An overview of CMIP5 and the experiment design, *Bull. Am. Meteorol. Soc.*, *93*, 485–498.

Tolman, H. L. (2002), Alleviating the garden sprinkler effect in wind wave models, *Ocean Modell.*, *4*, 269–289.

Tolman, H. L. (2014), *User Manual and System Documentation of WAVEWATCH III, Version 4.18*. Environmental Modeling Center Marine Modeling and Analysis Branch, U. S. Department of Commerce National Oceanic and Atmospheric Administration National Weather Service National Centers for Environmental Prediction 5200 Auth Road Camp Springs, MD.

Wang, X. L., and V. R. Swail (2006), Climate change signal and uncertainty in projections of ocean wave heights, *Clim. Dyn.*, *26*, 109–126, doi:10.1007/s00382-005-0080-x.

Wang, X. L., Y. Feng, and V. R. Swail (2014), Changes in global ocean wave heights as projected using multimodel CMIP5 simulations, *Geophys. Res. Lett.*, *41*, 1026–1034, doi:10.1002/2013GL058650.

Wehner, M., Prabhat, K. A. Reed, D. Stone, W. D. Collins, and J. Bacmeister (2015), Resolution dependence of future tropical cyclone projections of CAM5.1 in the U.S. CLIVAR hurricane working group idealized configurations, *J. Clim.*, *28*, 3905–3925, doi:10.1175/JCLI-D-14-00311.1.

Wehner, M. F., et al. (2014), The effect of horizontal resolution on simulation quality in the Community Atmospheric Model, CAM5.1, *J. Adv. Model. Earth Syst.*, *6*, 980–997, doi:10.1002/2013MS000276.